weakness called "steroid myopathy" [5], far less attention has been paid to this condition than GIO. We suspected that myopathy and increased risk of falling might also be responsible for the increased risk of fracture. The patients included in this study received glucocorticoid treatment for the first time, and the patients that received higher doses of glucocorticoid were exclusively studied. The protocol was so determined because we considered that it is a suitable model to study the initial effects of high-dose glucocorticoid on the musculoskeletal system.

Materials and methods

Thirty-three patients hospitalized at the Kyoto University Hospital and scheduled to receive intensive glucocorticoid therapy were recruited in this study (Table 1). None of the patients had received glucocorticoid treatment before. Five patients were male (54.0 ± 7.6 years old), and 28 were female (38.9 ± 16.4 years old). "Intensive glucocorticoid therapy" was arbitrarily defined as the daily dose of glucocorticoid ≥40 mg of predonisolone equivalent. Nineteen patients received intravenous pulse treatment followed by oral glucocorticoid treatment. Fourteen patients received only oral glucocorticoid treatment. Their underlying diseases are as follows, with the number of subjects in parentheses: Graves' ophthamopathy (8), dermatomyositis (DM), polymyositis (PM) and mixed connective disorder (MCTD) (9), systemic lupus erythematodes (SLE) (16) and nephrotic syndrome (NS) [2]. Bone mineral density (BMD) and body composition were measured before and 2 months after initiating the glucocorticoid therapy. These measurements were performed with dual energy X-ray absorptiometry (DXA) (QDR-2000; Hologic, Waltham, Mass.) by a single examiner. BMDs were measured for the lumbar spine (L2–4), femoral neck and whole body. From the whole body measurement, the following parameters of body composition were obtained: lean body mass (LBM), fat mass (FAT) and bone mineral content (BMC).

Table 1 Patient characteristics

Number of patients	33		
Sex and age	Male	5	(54.0 ± 7.6 years old)
	Female	28	(38.9 ± 16.4 years old)
Underlying diseases	Systemic lupus erythematosus	(16)	
	Myositis	(9)	
	Graves' opthalmopathy	(8)	
Route of administration	Intravenous pulse + oral	(19)	
	Oral	(14)	

Results

High-dose glucocorticoid treatment for 2 months caused significant BMD loss at all three sites measured in the present study (Table 2). Of these three sites, the lumbar spine showed the greater percentage of BMD loss (–2.87%) compared to the femoral neck (–1.37%) and whole body (–1.10%). These differences were highly statistically significant by Fisher's PLSD.

The effect of high-dose glucocorticoid treatment on body composition was also studied (Table 3A). Two cases with nephrotic syndrome were excluded from the statistical analysis because the existence of severe edema is likely to interfere with the measurement of body composition. The initial body mass index (BMI) of the patients was 20.07 ± 3.06 kg/m^2, which did not significantly deviate from the standard BMI value of 22. Intensive glucocorticoid treatment for 2 months significantly decreased the BMI to 19.19 ± 2.83 kg/m^2 ($P < 0.05$).

BMC and LBM significantly decreased after glucocorticoid treatment (Table 3A). In contrast, fat mass (FAT) significantly increased. When expressed as %FAT, that is the ratio of FAT divided by body weight, the change was more pronounced. Thus, %FAT before treatment was 22.72 ± 6.22%, and it increased to 25.26 ± 5.65% after treatment ($P < 0.001$).

To exclude possible interference by the pre-existing myositis, data were also analyzed in 24 patients, excluding the cases with muscle involvement (DM/PM/MCTD) (Table 3B). The results were similar to the ones from the whole 33 cases. Thus BMI, BMC and LBM significantly decreased after the treatment. Although FAT after treatment was not statistically different from the pre-treatment value, %FAT after treatment was significantly higher than that before treatment.

The total dosage of glucocorticoid within 2 months ranged from 1,000 to 4,000 mg in cases with oral glucocorticoid treatment, and from 4,500 to 12,000 mg in cases with intravenous pulse treatment. Total glucocorticoid dosage correlated with none of the parameters in the present study, such as BMI, LBM and fat mass (data not shown).

Discussion

Recently, van Staa et al. clearly demonstrated that glucocorticoid use is a significant risk factor for both vertebral and nonvertebral fractures [2]. Their study is an exceptionally large-scale study from the UK including over 240,000 subjects in both control and glucocorticoid groups. Their reports have some important clinical implications. First, they found that even a small dosage of glucocorticoid use for a short duration of time significantly increased the risk of fracture. Until recently, glucocorticoid use was considered to be a risk factor for osteoporosis when the average daily dosage was greater

Table 2 Changes in bone mineral density after 2 months of high-dose glucocorticoid treatment

	Pretreatment	Post-treatment	*P* value
Lumbar spine (L2–4)	0.94±0.17	0.91±0.17	<0.0001
Femoral neck	0.735±0.123	0.725±0.125	<0.01
Whole body	1.031±0.111	1.019±0.111	<0.001

than or equal to the predonisolone equivalent of 7.5 mg and the duration was >6 months [6]. According to van Staa et al., however, fracture risk was already increased at as early as 3 months after starting the glucocorticoid treatment, and even a daily dosage of less than 2.5 mg predonisolone equivalent was associated with increased risk of vertebral fracture [2]. Another important implication was that glucocorticoid treatment was unequivocally proven to be a risk factor for fracture. The current concept holds that the reduction of fracture risk should be the endpoint in the treatment of osteoporosis, the increase of BMD being only a surrogate endpoint [7]. Thus, it is a landmark study in that fracture was the endpoint in the study of GIO.

In the current study, only 2 months of high-dose glucocorticoid treatment markedly decreased BMD in all three sites measured: the lumbar spine, femoral neck and whole body. The BMD decrease was the greatest in the lumbar spine compared to the femoral neck and whole body. These differences are likely to be due to the variable composition of each bone [8]. Thus, the lumbar spine is mainly composed of trabecular bone, and both cortical and trabecular bones contribute to the femoral neck BMD. Since approximately 70% of total bone volume is composed of cortical bone, cortical bone volume is the major determinant of total body BMD. Therefore, these results suggest that trabecular bone is mainly affected by intensive glucocorticoid treatment, which is in accordance with the previous reports [6].

Although glucocorticoid affects various aspects of skeletal homeostasis, its major effect is considered to be the suppression of bone formation, which is mainly exerted through inducing apoptosis in osteoblasts and osteocytes, and suppressing local IGF-1 production [9, 10]. Although glucocorticoid is known to decrease intestinal calcium absorption, the effect is usually only modest and does not cause marked secondary hyperparathyroidism. Glucocorticoid also increases urinary calcium excretion by inhibiting tubular calcium reabsorption. With regard to bone resorption, glucocorticoid treatment is reported to enhance bone resorption transiently by inducing RANKL and suppressing OPG [9, 10].

Despite the significant detrimental effects of glucocorticoid on BMD, it is not likely to be the sole explanation for the glucocorticoid-induced increase in the fracture rate. The fracture risk in GIO has been reported to be either altered [11] or unaltered [12]. A recent paper by Wallch, however, strongly favors the notion that fracture occurs at higher BMD values in GIO than in postmenopausal osteoporosis [4]. In their report, which is part of the risedronate trial on GIO, the vertebral fracture rate was as high as 16%, whereas lumbar BMD was only modestly decreased, the average T score being −1.2. Van Staa et al. suggested three mechanisms for the increased fracture rate in GIO [2]: the apoptosis of osteoblasts and osteocytes, the marked alteration in bone turnover and non-skeletal mechanisms such as falling. Glucocorticoid is known to alter the body composition greatly. Muscle weakness called "steroid myopathy" and central obesity are well-known complications of glucocorticoid treatment [5], and muscle weakness is by no doubt one of the major risk factors of falling. In this study, body composition was evaluated by DXA, since it is considered to be a standard method for the evaluation of body composition as well as for BMD measurement [13]. LBM significantly decreased, and FAT increased in a reciprocal fashion in within only 2 months, Therefore, the percentage of fat (%FAT) increased by approximately 10%. Although vertebral fracture, which is the most prevalent fracture in GIO, is not associated with falling [10], an increased rate of falling would lead to the increased risk of hip and wrist fractures. Thus, our current finding may explain at least partially the increased fracture risk in glucocorticoid treatment.

Another implication of the current findings would be the rapidity with which bone loss occurs after initiating

Table 3 Changes in body composition after 2 months of high-dose glucocorticoid treatment. *A* and *B* show the data from whole subjects and data from patients excluding ones with myositis, respectively. BMC, LBM and FAT are expressed in kg. %FAT is the ratio of fat to body weight

	Pretreatment	Post-treatment	*P* value
A			
Body mass index (BMI)	20.07±3.06	19.19±2.83	<0.05
Body composition			
Bone mineral content (BMC)	1.94±0.38	1.88± 0.37	<0.001
Lean body mass (LBM)	37.30±6.80	34.26± 5.00	<0.0001
Fat mass (FAT)	11.66±4.00	12.47±3.95	<0.05
%FAT	22.72±6.22	25.26±5.65	<0.001
B			
Body mass index (BMI)	20.00±3.37	19.28±3.05	<0.05
Body composition			
Bone mineral content (BMC)	1.89±0.34	1.84±0.33	<0.001
Lean body mass (LBM)	35.52±6.37	33.33±4.79	<0.005
Fat mass (FAT)	12.03±4.51	12.44±4.22	NS
% FAT	23.89±6.75	25.60±6.22	<0.05

intensive glucocorticoid treatment. It is now established that even low dose glucocorticoid treatment increases the fracture risk. Vestergaard et al. reported that even a limited daily dose of glucocrticoid (more than an average dose of 71 μg predonisolone per day) was associated with an increased risk of hip fracture [14]. In the guideline for GIO recently published by the UK, it is recommended that BMD measurement should be considered for patients committed or exposed to oral glucocorticoid for more than 3 months, irrespective of the glucocorticoid dose [15]. These reports, together with the current findings, strongly suggest that attention should be paid to the prevention as well as the treatment of GIO.

These changes are unlikely to be secondary to hospitalization or due to underlying disease alone. First, increased %FAT in face of decreased body weight is quite unlikely to occur as the result of underlying disease or the subsequent malnutrition. Moreover, when the subgroup of patients with euthyroid Graves' disease was separately analyzed, these changes in body composition and biochemical parameters were similarly observed (data not shown). These patients have inflammatory changes only in their extraocular muscle and do not have any limitation in their daily activities except for double vision. Therefore, these marked changes are probably due to the intensive glucocorticoid treatment rather than other factors. Additionally, the patients' BMD was not markedly decreased before treatment. Since reference data for whole body BMD using QDR-2000 in the Japanese population is not available, we have not expressed our data in Z score. The young adult mean (YAM) for lumbar spine BMD in Japanese women is 1.011 ± 0. The YAM for the femoral neck BMD is 0.787 ± 0.109 for women and 0.863 ± 0.127 for men. Thus, it is quite unlikely that underlying diseases had adversely affected the subjects' skeletons before glucocorticoid treatment.

In summary, we have shown that intensive glucocorticoid treatment rapidly induces trabecular bone loss and lean body mass, both of which probably contribute to the recently reported rapid onset of increased fracture risk after initiating glucocorticoid treatment.

References

1. Saag KG, Koehnke R, Caldwell JR, Brasington R, Burmeister LF, Zimmerman B, Kohler JA, Furst DE (1994) Low dose long-term corticosteroid therapy in rheumatoid arthritis: an analysis of serious adverse events. Am J Med 96:115–123
2. van Staa TP, Leufkens HGM, Abenhaim L, Zhang B, Cooper C (2000) Use of oral corticosteroid and risk of fractures. J Bone Miner Res 15:993–1000
3. van Staa TP, Leufkens HG, Cooper C (2002) The epidemiology of corticosteroid-induced osteoporosis: a meta-analysis. Osteoporos Int 13:777–787
4. Wallach S, Cohen S, Reid DM, Hughes RA, Hosking DJ, Laan RF, Doherty SM, Maricic M, Rosen C, Brown J, Barton I, Chines AA (2000) Effects of risedronate treatment on bone density and vertebral fracture in patients on corticosteroid therapy. Calcif Tissue Int 67:277–285
5. Kanda F, Okuda S, Matsushita T, Takatani K, Kimura KI, Chihara K (2001) Steroid myopathy: pathogenesis and effects of growth hormone and insulin-like growth factor-I administration. Horm Res 56:S24–S28
6. American College of Rheumatology Task Force on Osteoporosis Guidelines (1996) Recommendations for the prevention and treatment of glucocorticoid-induced osteoporosis. Arth Rheum 39:1791–1801
7. Pearson D, Miller CG (eds) (2002) Clinical trials in osteoporosis. Springer, Heidelberg Germany New York
8. Bonnick SL, Lewis LA (2002) Bone densitometry for technologists. Humana Press, Totowa, NJ
9. Canalis E, Giustina A (2001) Glucocorticoid-induced osteoporosis: summary of a workshop. J Clin Endocrinol Metab 86:5681–5685
10. Canalis E, Delany AM (2002). Mechanism of glucocorticoid action in bone. Ann NY Acad Sci 966:73–81
11. Luengo M, Picado C, Del Rio L, Guanabens N, Monsterrat JM, Setoain J (1991) Vertebral fractures in steroid dependent asthma and involutional osteoporosis. Thorax 46:803–806
12. Selby PL, Halsey JP, Adams KRH, Klimiuk P, Knight SM, Pal B, Stewart IM, Swinson DR (2000) Corticosteroids do not alter the threshold for vertebral fracture. J Bone Miner Res 15:952–956
13. Houtkooper LB, Going SB, Sproul J, Blew RM, Lohman TG (2000) Comparison of methods for assessing body-composition changes over 1 year in postmenopausal women. Am J Clin Nutr 72:401–406
14. Vestergaard P, Olsen ML, Paaske Johnsen S, Rejnmark L, Toft Sorensen H, Mosekilde L. (2003) J Intern Med 254:486–493
15. Bone and Tooth Society, National Osteoporosis Society, Royal College of Physicians. (2002) Glucocorticoid-induced osteoporosis: guidelines for prevention and treatment. Royal College of Physicians, London

Endocrine Journal 2005, **52** (5), 551–557

Anaplastic Thyroid Carcinoma Associated with Graves' Disease

TAKAFUMI MAJIMA*,**, YASATO KOMATSU**, KENTARO DOI*, MICHIKA SHIGEMOTO*, CHIEKO TAKAGI*, ATSUSHI FUKAO***, MASATSUGU KOJIMA#, HISANOBU TAMAKI#, JUICHI ITO# AND KAZUWA NAKAO**

**Department of Endocrinology and Metabolism, Rakuwakai Otowa Hospital, Kyoto 607-8062, Japan*
***Department of Medicine and Clinical Science, Kyoto University Graduate School of Medicine, Kyoto 606-8507, Japan*
****Department of Psychosomatic Medicine, Rakuwakai Otowa Hospital, Kyoto 607-8062, Japan*
#Department of Otolaryngology - Head and Neck Surgery, Graduate School of Medicine, Kyoto University, Kyoto 606-8507, Japan

Abstract. This report concerns a 79-year-old woman with coexisting anaplastic thyroid carcinoma (ATC) and Graves' disease (GD). The patient was referred to our clinic because of palpitation and a palpable mass on the left side of her neck. Thyroid function tests showed hyperthyroidism with elevated thyroid-stimulating antibodies. Ultrasonography of the thyroid demonstrated an adenomatous nodule-like marcated nodule (27.6 × 26.5 × 36.4 mm) with cystic degeneration inside the left lobe. ^{123}I thyroid scintigraphic imaging showed a cold area corresponding to the nodule with continuous uptake in the remaining thyroid tissue despite suppressed TSH levels. These findings led to a diagnosis of GD. On the other hand, the thyroid nodule could not be definitely diagnosed even after fine needle aspiration biopsy (FNAB) which produced findings suggestive of both papillary thyroid carcinoma and ATC. Open biopsy of the nodule showed an ATC. Regional lymph node metastases as well as multiple lung metastases, which could not be found at the initial visit, had been already developed by that time. Our case is pathophysiologically interesting because it suggests that GD or thyroid-stimulating antibodies (TSAb) may stimulate malignant transformation of differentiated carcinoma. It is also clinically important because it indicates that all thyroid nodules, particularly palpable cold nodules, associated with GD require careful management to detect malignancy because they are at higher risk of harboring malignancy.

Key words: Anaplastic thyroid carcinoma, Graves' disease, Thyroid-stimulating antibody, Anaplastic transformation
(*Endocrine Journal* **52**: 551–557, 2005)

THYROID nodules occur commonly in association with Graves' disease (GD) and more frequently than in the general population [1, 2]. Since 2.3% to 45.8% of these nodules accompanying GD have been reported to be malignant [1, 2] and the aggravated aggressiveness of thyroid cancer in GD has been described in numerous reports [3–9], the presence of thyroid nodules in conjunction with GD should cause concern about coexistent thyroid malignancy. However, how to preoperatively diagnose malignancy in GD-associated nodules with certainty has not yet been fully established [2, 10–13].

On the other hand, anaplastic thyroid carcinoma (ATC) is not common, accounting for only about 2% of all thyroid carcinomas, but it is one of the most aggressive malignant diseases with very poor prognosis [14, 15]. To the best of our knowledge, only six case reports, including the one presented here, on ATC associated with hyperthyroidism have ever been published [3, 4, 16, 17], and whether GD affects the initiation, promotion or prognosis of ANA remains obscure.

In this report, we present a rare case of ATC associated with GD.

Received: March 23, 2005
Accepted: May 16, 2005
Correspondence to: Takafumi MAJIMA, M.D., Department of Endocrinology and Metabolism, Rakuwakai Otowa Hospital, 2 Otowa Chinji-cho, Yamashina-ku, Kyoto 607-8062, Japan

Case Report

A 79-year-old Japanese woman was first referred to the Otowa Clinic in March 2004 because of palpitation, weight loss, and a painless mass on the left side of the neck. She had noticed the enlarged neck mass a few weeks earlier, but did not complain of compressive neck symptoms, dysphagia, hoarseness, or shortness of breath. She had lost 3 kg of body weight (from 51 kg to 48 kg) without loss of appetite over the previous 3 months. Other signs or symptoms suggestive of hyperthyroidism were not present. She had neither a family history of thyroid diseases nor a past history of radiation of the head or neck.

Physical examination showed her blood pressure and pulse to be normal. A golfball-sized, painless, and rather hard mass (approximately 4 cm in diameter) with a smooth surface was palpated on the anterior left side of the neck. No lymph nodes were palpable in the neck or supraclavicular region and other physical examination results were unremarkable.

Ultrasonography of the thyroid showed a marcated nodule containing cystic degeneration and measuring 27.6 × 26.5 × 36.4 mm (Fig. 1). Neck computed tomography (CT) scan showed some tracheal deviation to the right without narrowing of the airway, but neither of these imaging procedures produced any remarkable findings in the right thyroid lobe or lymph node swellings.

Routine laboratory data showed no abnormalities (CRP <0.24 mg/dl) except a somewhat elevated WBC 8100/μl with a slight increase in the neutrophil ratio (65.3%) and a decreased lymphocyte ratio (27.2%). However, thyroid function tests showed elevated free triiodothyronine (T3) of 4.88 pg/ml (reference range: 2.30–4.30 pg/ml) and free thyroxine (T4) of 2.53 ng/dl (reference range: 0.90–1.70 ng/dl), and virtually undetectable thyroid-stimulating hormone (TSH) at <0.005 μIU/ml (reference range: 0.500–5.00 μIU/ml). Serum thyroglobulin was 140.6 ng/ml (reference range: <30 ng/ml), and thyroid-stimulating antibody (TSAb), TSH receptor antibodies (TRAb), anti-thyroglobulin (TgAb) and anti-thyroperoxidase (TPOAb) antibodies were all elevated at 203.0% (reference range: <180%), 42.4% (reference range: <15%), 2.00 U/ml (reference range: <0.3 U/ml), and 73.3 U/ml (reference range: <0.3 U/ml), respectively.

A thyroid iodine-123 (^{123}I) scintigram after an iodine restricted diet for 7 days showed a cold area corresponding to the thyroid nodule, with maintained uptake in the remaining thyroid tissue although TSH was reduced to below the level of sensitivity (Fig. 2). Three-hour and 24-hour radioactive iodine thyroid uptakes were 5.63% (reference range: 5–15%) and 29.61% (reference range: 10–40%), respectively, although compliance with the restricted diet could not be assured because she was instructed as an outpatient at her request.

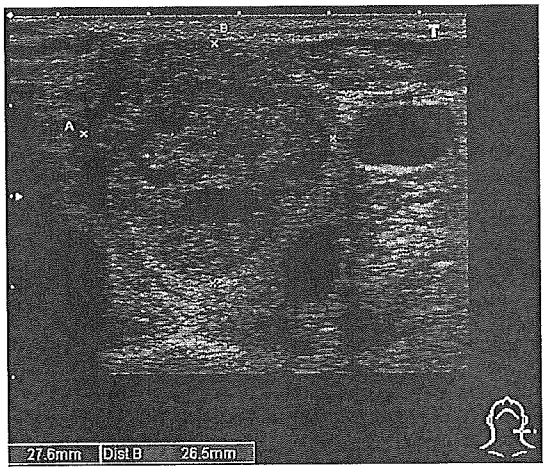

A

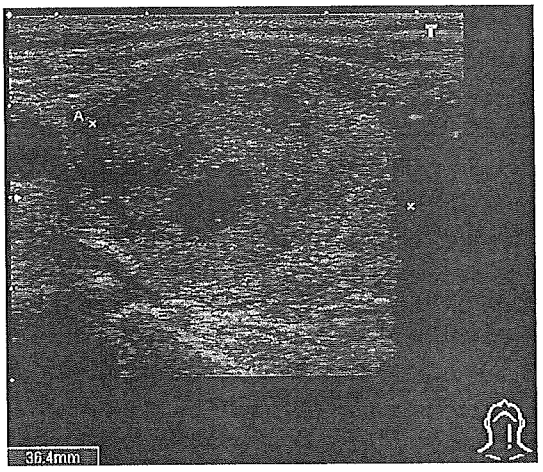

B

Fig. 1. Ultrasonography of the left thyroid lobe. (A) Horizontal section. (B) Sagittal section.

Our diagnosis was hyperthyroidism resulting from GD, and we began treating it with an anti-thyroid drug (methimazole, 15 mg/day). Since the nodule could not be diagnosed, however, we recommended fine needle aspiration biopsy (FNAB) to determine whether the nodule was malignant or not, but she refused and

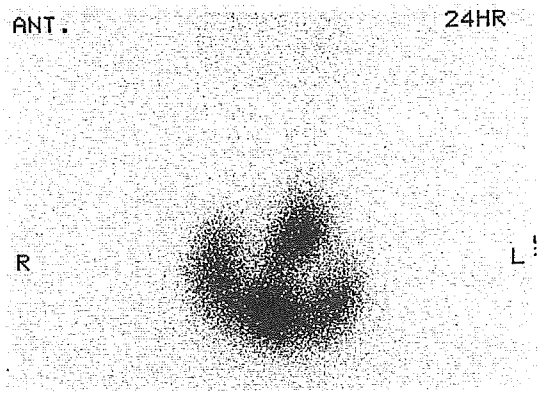

Fig. 2. Thyroid ^{123}I scintigram demonstrating a cold area corresponding to the thyoid nodule in the left lobe. The rest of the gland shows maintained uptake despite TSH suppressed below sensitivity.

stopped coming to our clinic. Instead, she attended the department of otorhinolaryngology of Kyoto University Hospital, where FNAB of the nodule was performed on 24 June 2004, showing Papanicolaou V. Atypical cells were found in biopsy specimens from the nodule, some of which had large nuclei with a pale ground-glass appearance or with intranuclear inclusion. Although the nodule could be interpreted as a papillary adenocarcinoma, the degree of pleomorphism was substantially higher than that generally seen in association with a differentiated carcinoma, and the atypical cells were isolated from each other, indicating an anaplastic thyroid carcinoma. The results of the FNAB showed the nodule to be malignant, but its histological type could not be diagnosed accurately.

Open biopsy of the nodule was thus performed in July 2004, and microscopic examination found marked pleomorphisms without duct-like configurations anywhere in the nodule. There were numerous giant cells, some of which contained multiple nuclei, against a background of some spindle cells and a scattering of neutrophils (Fig. 3). The nodule was therefore diagnosed as ATC. The biopsied tissue specimens contained only malignant cells and no benign or hyperplastic cells suggestive of GD.

By that time, the nodule had grown into a huge mass incorporating surrounding lymph node swellings, and chest roentgenography and CT showed findings suggesting multiple lung metastases. Furthermore, thyroid function declined to below the reference range without medication, probably because malignant tissue had mostly replaced the thyroid tissue associated with GD

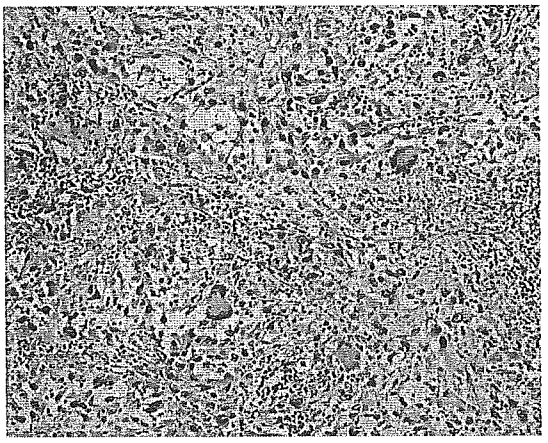

A

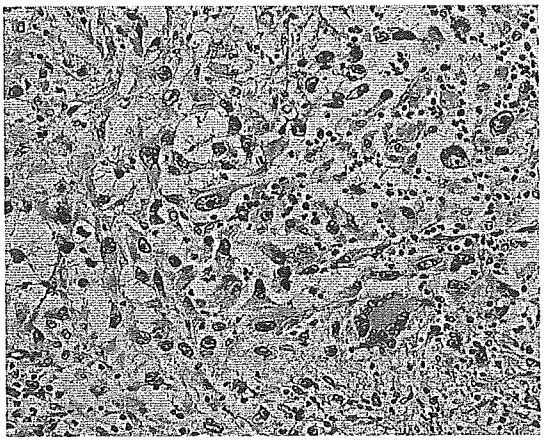

B

Fig. 3. Histologic appearance of the thyroid tumor demonstrating marked pleomorphism without duct-like configuration. There were numerous giant cells, some of which contained multiple nuclei, against a background of some spindle cells and a scattering of neutrophils. (A) Hematoxylin-eosin stain; ×100. (B) Hematoxylin-eosin stain; ×200.

or because TSH binding inhibitor immunogloblins (TBII) might have emerged although not measured, so that the patient needed levothyroxine (L-T4) replacement therapy (75 μg/day). She was diagnosed as no longer curable with surgery, and was treated in vain with oral chemotherapy. In December 2004, she died of respiratory failure probably due to airway narrowing.

Discussion

Our patient with GD presented with a solitary pal-

pable thyroid nodule, which revealed ATC. It has been reported that a palpable thyroid nodule occurs in approximately 12.8% to 26.9% of patients with GD [11, 18–20], and in 33.6% when detected ultrasonographically [21]. This comparatively high frequency of thyroid nodule occurrence has therefore raised clinical concern about the co-existence of thyroid malignancy [11].

The reported frequencies of thyroid cancer in patients with GD are reviewed in Table 1, ranging from 0% to as high as 12.5% [5–13, 18–43]. In comparison, thyroid cancer is an infrequent malignant tumor in the general population, with an incidence ranging from 0.5 to 10 per 100,000 [1]. Furthermore, when a nodule is detected in association with GD, the malignancy rate of the nodule is reportedly 10% to 17.1% [10, 11, 20, 43], and becomes higher if the patient is older [13], or if the nodule is palpable [7, 35, 40], solitary [22], or scintigraphically cold [7, 20, 41, 43] whereas carcinoma in a hot nodule is extremely rare [22, 44]. Therefore, it would appear that the nodule in our case had potentially high risk of malignancy. It is regrettable that our ef-

Talbe 1. Published series of thyroid cancer in patients with Graves' disease

Authors and Year		Patients with GD	Patients with GD with Cancer		Histology of Cancer		
					Papillary	Follicular	Other
		(n)	(n)	(%)	(n)	(n)	(n)
Beahrs *et al.*[23]	51	3029	14	0.46		not shown	
Sokal[24]	54	13868	21	0.15		not shown	
Shaprio *et al.*[25]	70	172	15	8.7	10	10	1
Dobyns *et al.*[18]	74	30343	47	0.15	33	7	7
Hancock *et al.*[26]	77	451	7	1.5	4	3	
Wahl *et al.*[27]	82	178	2	1.1	2		
Farbota *et al.*[28]	85	117	6	5.1	4	2	
Behar *et al.*[5]	86	194	10	5.2		not shown	
Pacini *et al.*[19]	88	86	6	6.9	2	4	
Rieger *et al.*[29]	89	64	0	0.0		0	
Ozaki *et al.*[6]	90	743	19	2.6	15	4	
Belfiore *et al.*[7]	90	132	13	9.8		not shown	
Hales *et al.*[30]	92	886	16	1.8	15	1	
Chou *et al.*[31]	93	674	10	1.5	9	1	
Terzioglu *et al.*[32]	93	33	2	6.1	2		
Soh and Park[33]	93	545	11	2.2	10	1	
Kasuga *et al.*[34]	93	847	36	4.3	30	6	
Thakur *et al.*[35]	95	49	4	8.2	3	1	
Miccoli *et al.*[36]	96	140	13	9.3	13		
Pomorski *et al.*[37]	96	704	3	0.4	1	2	
Carnell and Valente[20]	98	468	6	1.3	5	1	1
Pellegriti *et al.*[8]	98	450	36	8.0		not shown	
Cantalamessa *et al.*[21]	99	315	1	0.32		not shown	
Chao *et al.*[9]	99	2934	30	1.0		not shown	
Vaiana *et al.*[38]	99	108	7	6.4	7		
Ruggieri *et al.*[39]	99	8	1	12.5	1		
Kraimps *et al.*[10]	00	557	21	3.8	20	1	
Mishra and Mishra[11]	01	130	8	6.2	5	1	2
Zanella *et al.*[40]	99	38	2	5.3	1	1	
Stocker *et al.*[41]	02	325	6	1.9	6		
Lin *et al.*[22]	03	42	4	9.5	1	2	1
Gabriele *et al.*[12]	03	64	0	0.0		0	
Gerenova *et al.*[42]	03	103	8	7.8	8		
Chao *et al.*[43]	04	3112	61	2.0	58	1	2
Kim *et al.*[13]	04	245	8	3.3	8		

forts to persuade her to undergo FNA ended in failure.

Most carcinomas associated with GD appear to be small, micro-papillary carcinomas [43]. Indeed, among the 336 carcinomas whose histologic type was shown in the previous studies reviewed by us (Table 1), most of them, 273 carcinomas, were papillary whereas no ATC was found. To the best of our knowledge, only 6 case reports, including the one presented here, of ATC associated with hyperthyroidism have ever been published [3, 4, 16, 17]. Among them, there was only one case report by Fujikawa *et al.* [4] that clearly showed association of GD and ATC. In our case, TSAb may have promoted the anaplastic transformation of the papillary carcinoma, as was also hypothesized by Fujikawa *et al.* [4]. While it has often been postulated that TSAb increases aggressiveness in well-differentiated thyroid cancer, whether ATC in GD is more aggressive or not and whether TSAb affects the behavior of ATC are unclear [1, 2, 4] because of their rare association.

The reported risk factors for ATC are age, gender, acute symptoms, larger tumor size, distant metastasis, and leukocytosis [15], which are important but not quite enough to establish suspicion of ATC at an early stage. Although there have been some case reports showing ATC producing granulocyte colony-stimulating factor (G-CSF) or parathyroid hormone-related protein (PTH-rp) [14, 45], neither higher G-CSF nor higher PTH-rp was found in our study. It is widely believed that multiple incidents of damage to the genome including p53 mutations lead to anaplastic transformation of differentiated thyroid cancer [14], but, unfortunately, genetic testing cannot be performed with ease and was not done in our study. Takano [46] has recently suggested that the remnants of fetal thyroid cells constitute a risk factor for anaplastic transformation, although they were also difficult to identify. Further studies are warranted to clarify risk factors for ATC, including whether TSAb or GD itself is a risk factor for anaplastic transformation.

Surgical treatment [2, 10, 11, 22, 43], or at least a low threshold for surgical referral [1, 2, 20, 43], is considered by many to be the most appropriate modality for thyroid nodules associated with GD, because there are no pre-operative investigations that can exclude malignancy with certainty in spite of the high risk of malignancy in those nodules and their aggressive behavior [13]. In addition, some clinical studies have found that complete removal of the primary lesion of ATC at an early stage has been associated with better prognosis [15]. Therefore, it might have been better to decide to perform thyroidectomy at the initial visit in this case, which might have rescued the patient.

In conclusion, our case is pathophysiologically interesting because it suggests that GD or TSAb may stimulate malignant transformation of differentiated carcinoma. It is also clinically important because it indicates that all thyroid nodules, particularly non-occult (>10 mm) cold nodules, associated with GD require careful and intensive management to detect malignancy because they are at higher risk of harboring malignancy.

References

1. Belfiore A, Russo D, Vigneri R, Filetti S (2001) Graves' disease, thyroid nodules and thyroid cancer. *Clin Endocrinol (Oxf)* 55: 711–718.
2. Stocker DJ, Burch HB (2003) Thyroid cancer yield in patients with Graves' disease. *Minerva Endocrinol* 28: 205–212.
3. Hayes FJ, Sheahan K, Heffernan A, McKenna TJ (1996) Aggressive thyroid cancer associated with toxic nodular goitre. *Eur J Endocrinol* 134: 366–370.
4. Fujikawa M, Okamura K, Sato K, Asano T, Yamasaki K, Hirata T, Ohta M, Mizokami T, Kuroda T, Fujishima M (1998) Anaplastic transformation of a papillary carcinoma of the thyroid in a patient with Graves' disease with varied activity of thyrotropin receptor antibodies. *Thyroid* 8: 53–58.
5. Behar R, Arganini M, Wu TC, McCormick M, Straus FH 2nd, DeGroot LJ, Kaplan EL (1986) Graves' disease and thyroid cancer. *Surgery* 100: 1121–1127.
6. Ozaki O, Ito K, Kobayashi K, Toshima K, Iwasaki H, Yashiro T (1990) Thyroid carcinoma in Graves' disease. *World J Surg* 14: 437–441.
7. Belfiore A, Garofalo MR, Giuffrida D, Runello F, Filetti S, Fiumara A, Ippolito O, Vigneri R (1990) Increased aggressiveness of thyroid carcinoma patients with Graves' disease. *J Clin Endocrinol Metab* 70: 830–835.
8. Pellegriti G, Belfiore A, Giuffrida D, Lupo L, Vigneri R (1998) Outcome of differentiated thyroid cancer in Graves' patients. *J Clin Endocrinol Metab* 83: 2805–2809.
9. Chao TC, Lin JD, Jeng LB, Chen MF (1999) Thyroid cancer with concurrent hyperthyroidism. *Arch Surg*

134: 130–134.
10. Kraimps JL, Bouin-Pineau MH, Mathonnet M, De Calan L, Ronceray J, Visset J, Marechaud R, Barbier J (2000) Multicentre study of thyroid nodules in patients with Graves' disease. *Br J Surg* 87: 1111–1113.
11. Mishra A, Mishra SK (2001) Thyroid nodules in Graves' disease: implications in an endemically iodine deficient area. *J Postgrad Med* 47: 244–247.
12. Gabriele R, Letizia C, Borghese M, De Toma G, Celi M, Izzo L, Cavallaro A (2003) Thyroid cancer in patients with hyperthyroidism. *Horm Res* 60: 79–83.
13. Kim WB, Han SM, Kim TY, Nam-Goong IS, Gong G, Lee HK, Hong SJ, Shong YK (2004) Ultrasonographic screening for detection of thyroid cancer in patients with Graves' disease. *Clin Endocrinol (Oxf)* 60: 719–725.
14. Sugitani I, Kasai N, Fujimoto Y, Yanagisawa A (2001) Prognostic factors and therapeutic strategy for anaplastic carcinoma of the thyroid. *World J Surg* 25: 617–622.
15. Kihara M, Miyauchi A, Yamauchi A, Yokomise H (2004) Prognostic factors of anaplastic thyroid carcinoma. *Surg Today* 34: 394–398.
16. Mangla JC, Rastogi GK, Pathak IC (1967) Anaplastic carcinoma of the thyroid complicating severe thyrotoxicosis. *J Indian Med Assoc* 49: 286, 291–292.
17. Oppenheim A, Miller M, Anderson GH Jr, Davis B, Slagle T (1983) Anaplastic thyroid cancer presenting with hyperthyroidism. *Am J Med* 75: 702–704.
18. Dobyns BM, Sheline GE, Workman JB, Tompkins EA, McConaley WM, Becker DV (1974) Malignant and benign neoplasms of the thyroid in patients treated for hyperthyroidism. *J Clin Endocrinol Metab* 38: 976–998.
19. Pacini F, Elisei R, Di Coscio GC, Anelli S, Macchia E, Concetti R, Miccoli P, Arganini M, Pinchera A (1988) Thyroid carcinoma in thyrotoxic patients treated by surgery. *J Endocrinol Invest* 11: 107–112.
20. Carnell NE, Valente WA (1998) Thyroid nodules in Graves' disease: classification, characterization, and response to treatment. *Thyroid* 8: 647–652.
21. Cantalamessa L, Baldini M, Orsatti A, Meroni L, Amodei V, Castagnone D (1999) Thyroid nodules in Graves' disease and the risk of thyroid carcinoma. *Arch Intern Med* 159: 1705–1708.
22. Lin CH, Chiang FY, Wang LF (2003) Prevalence of thyroid cancer in hyperthyroidism treated by surgery. *Kaohsiung J Med Sci* 19: 379–384.
23. Beahrs OH, Pemberton Jde J, Black BM (1951) Nodular goiter and malignant lesions of the thyroid gland. *J Clin Endocrinol Metab* 11: 1157–1165.
24. Sokal JE (1954) Incidence of malignancy in toxic and nontoxic nodular goiter. *JAMA* 154: 1321–1325.
25. Shapiro SJ, Friedman NB, Perzik SL, Catz B (1970) Incidence of thyroid carcinoma in Graves' disease. *Cancer* 26: 1261–1270.
26. Hancock BW, Bing RF, Dirmikis SM, Munro DS, Neal FE (1977) Thyroid carcinoma and concurrent hyperthyroidism: a study of ten patients. *Cancer* 39: 298–302.
27. Wahl RA, Goretzki P, Meybier H, Nitschke J, Linder M, Roher HD (1982) Coexistence of hyperthyroidism and thyroid cancer. *World J Surg* 6: 385–390.
28. Farbota LM, Calandra DB, Lawrence AM, Paloyan E (1985) Thyroid carcinoma in Graves' disease. *Surgery* 98: 1148–1153.
29. Rieger R, Pimpl W, Money S, Rettenbacher L, Galvan G (1989) Hyperthyroidism and concurrent thyroid malignancies. *Surgery* 106: 6–10.
30. Hales IB, McElduff A, Crummer P, Clifton-Bligh P, Delbridge L, Hoschl R, Poole A, Reeve TS, Wilmshurst E, Wiseman J (1992) Does Graves' disease or thyrotoxicosis affect the prognosis of thyroid carcinoma. *J Clin Endocrinol Metab* 75: 886–889.
31. Chou FF, Sheen-Chen SM, Chen YS, Chen MJ (1993) Hyperthyroidism and concurrent thyroid cancer. *Int Surg* 78: 343–346.
32. Terzioglu T, Tezelman S, Onaran Y, Tanakol R (1993) Concurrent hyperthyroidism and thyroid carcinoma. *Br J Surg* 80: 1301–1302.
33. Soh EY, Park CS (1993) Diagnostic approach to thyroid carcinoma in Graves' disease. *Yonsei Med J* 34: 191–194.
34. Kasuga Y, Sugenoya A, Kobayashi S, Masuda H, Iida F (1993) The outcome of patients with thyroid carcinoma and Graves' disease. *Surg Today* 23: 9–12.
35. Thakur S, Sharma AK, Agarwal A, Mishra SK, Bhatia E (1995) Carcinoma in Graves' disease. *J Assoc Physicians India* 43: 600–601.
36. Miccoli P, Vitti P, Rago T, Iacconi P, Bartalena L, Bogazzi F, Fiore E, Valeriano R, Chiovato L, Rocchi R, Pinchera A (1996) Surgical treatment of Graves' disease: subtotal or total thyroidectomy? *Surgery* 120: 1020–1024.
37. Pomorski L, Cywinski J, Rybinski K (1996) Cancer in hyperthyroidism. *Neoplasma* 43: 217–219.
38. Vaiana R, Cappelli C, Perini P, Pinelli D, Camoni G, Farfaglia R, Balzano R, Braga M (1999) Hyperthyroidism and concurrent thyroid cancer. *Tumori* 85: 247–252.
39. Ruggieri M, Scocchera F, Genderini M, Mascaro A, Luongo B, Paolini A (1999) Hyperthyroidism and concurrent thyroid carcinoma. *Eur Rev Med Pharmacol Sci* 3: 265–268.
40. Zanella E, Rulli F, Sianesi M, Sciacchitano S, Danese D, Pontecorvi A, Farinon AM (2001) Hyperthyroidism with concurrent thyroid cancer. *Ann Ital Chir* 72: 293–297.
41. Stocker DJ, Foster SS, Solomon BL, Shriver CD, Burch HB (2002) Thyroid cancer yield in patients with Graves' disease selected for surgery on the basis of

cold scintiscan defects. *Thyroid* 12: 305–311.
42. Gerenova J, Buysschaert M, de Burbure CY, Daumerie C (2003) Prevalence of thyroid cancer in Graves' disease: a retrospective study of a cohort of 103 patients treated surgically. *Eur J Intern Med* 14: 321–325.
43. Chao TC, Lin JD, Chen MF (2004) Surgical treatment of thyroid cancers with concurrent Graves disease. *Ann Surg Oncol* 11: 407–412.
44. Majima T, Doi K, Komatsu Y, Itoh H, Fukao A, Shigemoto M, Takagi C, Corners J, Mizuta N, Kato R, Nakao K (2005) Papillary thyroid carcinoma without metastases manifesting as an autonomously functioning thyroid nodule. *Endocr J* 52: 309–316.
45. Iwai H, Ohno Y, Aoki N (2004) Anaplastic thyroid carcinoma with humoral hypercalcemia of malignancy (HHM): an autopsy case report. *Endocr J* 51: 303–310.
46. Takano T (2004) Fetal cell carcinogenesis of the thyroid: a hypothesis for better understanding of gene expression profile and genomic alternation in thyroid carcinoma. *Endocr J* 51: 509–515.

Available online at www.sciencedirect.com
SCIENCE DIRECT
Regulatory Peptides 132 (2005) 17–22
REGULATORY PEPTIDES
www.elsevier.com/locate/regpep

Expression of the adrenomedullin gene in adipose tissue

Takuo Nambu, Hiroshi Arai *, Yasato Komatsu, Akihiro Yasoda, Kenji Moriyama, Naotetsu Kanamoto, Hiroshi Itoh, Kazuwa Nakao

Department of Medicine and Clinical Science Kyoto University Graduate School of Medicine 54 Shogoin-Kawahara-cho, Sakyo-ku, Kyoto 606-8507, Japan

Received 9 December 2004; received in revised form 16 February 2005; accepted 29 July 2005
Available online 8 September 2005

Abstract

Adrenomedullin (AM) is a potent vasodilating peptide originally isolated from human pheochromocytoma cells. This report concerns the expression and secretion of AM from adipose tissue. Northern blot analysis demonstrated marked expression of AM mRNA in mouse adipose tissue. Expression levels in adipose tissues were 2.5–3.2 times higher than in the kidney. AM mRNA level in mature adipocytes was 7.3 times higher than in the stroma–vascular fraction of adipose tissue. In mature adipocyte culture, time-dependent increase of AM peptide concentration in the culture medium was detected. AM expression was also detected in human subcutaneous adipose tissue. Adipose AM expression significantly increased in obesity mouse model, high-fat diet fed mice and ob/ob mice. These results suggest that adipose tissue, especially mature adipocytes, is major source of AM in the body, and that adipocyte-derived AM plays a pathophysiological role in obesity.

Keywords: Adrenomedullin; Adiopocyte; Fat; Obesity; ob/ob mice

1. Introduction

It has recently been suggested that adipose tissue is an endocrine organ. A wide variety of factors secreted from adipocytes, including leptin, TNF alpha, adiponectin, resistin and free fatty acid, are playing crucial roles in energy expenditure and glucose metabolism [1]. Adipocytes produce a host of vasoactive substances including angiotensinII [2], endothelin-1 [3], nitric oxide [4], prostacyclin [5] and natriuretic peptide [6]. Recent studies have suggested the paracrine/autocrine involvement of these molecules in the regulation of adipocyte growth and differentiation.

Adrenomedullin (AM) is a potent vasodilating peptide that was originally isolated from human pheochromocytoma cells [7]. Structural analysis indicates that AM belongs to the calcitonin gene-related peptide (CGRP) superfamily. AM and CGRP share a common receptor known as the calcitonin-receptor-like-receptor (CRLR). The ligand specificity of CRLR is regulated by the receptor-activity-modifying proteins (RAMPs), which is a family of proteins with a single transmembrane domain [8]. CRLR associated with RAMP1 acts as a CGRP receptor, while it binds to AM when coexpressed with RAMP2/3. It has been reported that AM-producing cells are distributed widely throughout the body, including the adrenal glands, lungs, heart and kidneys [9]. In vitro studies have demonstrated that vascular smooth muscle cells and endothelial cells secrete AM, and have suggested that the major source of AM in the body is the vascular wall [10].

We have previously reported that RAMPs are highly expressed in rat adipose tissue [11], and have posited the existence of an AM system in adipose tissue. The study reported here found massive expression of the AM gene in mouse and human adipose tissue, and its upregulation in obesity mouse models.

2. Materials and methods

2.1. Ethics

This study conforms to the policy of the Ethics Committee on Human Research of the Kyoto University Graduate School of Medicine, and written informed consent was obtained from all subjects.

Abbreviations: AM, adrenomedullin; CGRP, calcitonin gene-related peptide; RAMPs, receptor-activity-modifying protein; sv-f, stroma–vascular fraction; BAT, intrascapular brown adipose tissue; VEC, vascular endothelial cells; VSMC, vascular smooth muscle cells.

* Corresponding author. Tel.: +81 75 751 3181; fax: +81 75 771 9452.
E-mail address: hiroarai@kuhp.kyoto-u.ac.jp (H. Arai).

0167-0115/$ - see front matter © 2005 Elsevier B.V. All rights reserved.
doi:10.1016/j.regpep.2005.07.006

2.2. Mouse adipose tissue

Male C57BL/6 and ob/ob mice aged 14 weeks provided by Shionogi Research Laboratories (Osaka, Japan) were used in this study. They were treated in accordance with our institutional guidelines for animal research, housed in an animal room maintained at 24 °C with a 12:12-h light-dark cycle, fed a standard laboratory diet and given water ad libitum. The retroperitoneal, subcutaneous, omental, epididymal white adipose tissue, intrascapular brown adipose tissue (BAT), kidney, lung and heart were removed and stored at −80 °C until total RNA preparation.

2.3. Mature adipocytes

Murine mature adipocytes were isolated from subcutaneous adipose tissue of C3H/He mice (female, 8 months old) with a modificied version of the method of Rodbell [12]. In brief, the adipose tissue was minced and digested in a 0.2% collagenase solution at 37 °C for 1 h with constant shaking. The digested fluid was filtered through 100 μm nylon mesh and separated by centrifugation performed three times at 180 g for 5 min. Mature adipocytes appeared and were collected as a floating layer, while the sediment consisted of stroma–vascular fraction (sv-f).

2.4. Human adipose tissue

Human abdominal subcutaneous adipose tissue was obtained during plastic surgery after written permission had been obtained. Human kidney and lung mRNA were commercially available (Clontech Laboratories, Inc., Palo Alto, CA, USA).

2.5. RNA extraction and Northern blot analysis

Total RNA was extracted with TRIzol reagent (Invitrogen Co., Carlsbad, CA, USA). Northern blot analysis was performed as previously described using mouse and human AM cDNA as probes [11].

2.6. Measurements of AM released from isolated adipocytes

500 μl (2.5×10^5 cells) of isolated adipocytes from subcutaneous adipose tissue of ICR mouse (male, 12 weeks old) were incubated together with DMEM/H-12 (total volume: 500 μl) containing 10% fetal bovine serum in a CO_2 incubator for 24 h at 37 °C [13]. Aliquots of the incubation medium were removed at 6 and 24 h and stored at −20 °C for measurement of AM. The AM content in 100 μl of the incubation medium was determined by means of a radioimmunoassay (Phoenix Pharmaceuticals, Inc., Belmont, CA, USA).

2.7. TaqMan real time PCR

The quantitative real time RT-PCR was employed to examine the murine AM gene expression. Briefly, AM cDNA was synthesized with Superscript II reverse transcriptase (Gibco-BRL, St. Louis, MO, USA) and used as a template. The primers and probes for TaqMan PCR analysis were designed with primer-express software (Applied Biosystems, Foster City, CA, USA) as follows:

AM forward, 5′-CTCGCTGATGAGACGACAGTTC-3′,
AM reverse, 5′-CTCTGGCGGTAGCGTTTGAC-3′,
detection probe: 5′-CAGCAATCAGAGCGAAGCCCA-CATT-3′.

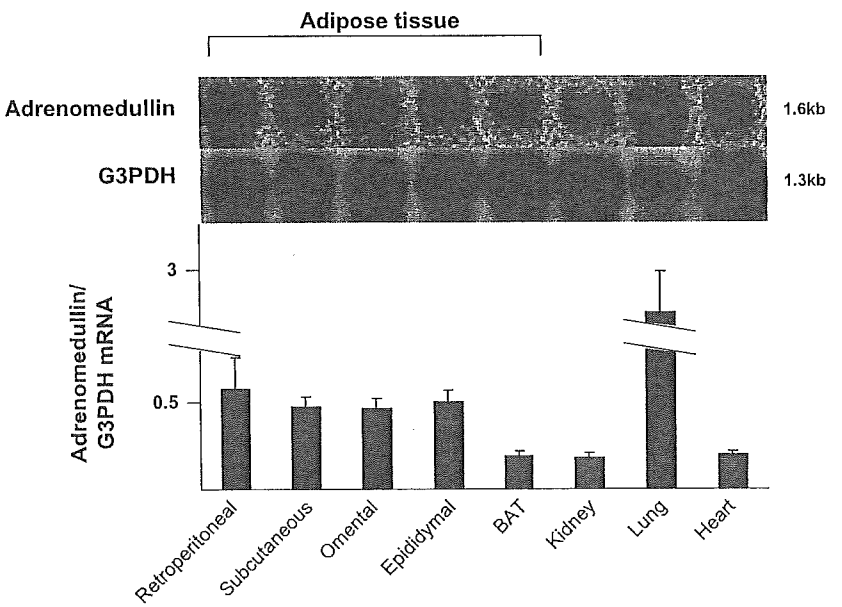

Fig. 1. Northern blot analysis of AM mRNA content of C57BL/6 mice. 10 μg of total RNA in each lane was electrophoresed and hybridized with mouse AM cDNA probes. The lower panel indicates hybridization with a G3PDH probe as an internal control. The ratio of AM to G3PDH mRNA is shown below. Bars represent mean ± S.E.M.

Rodent ribosomal 18S as an internal control was amplified using a commercially available kit (Applied Biosystems) at the same time. Thermal cycling was performed at 40 cycles of 95 °C for 15 s and of 60 °C for 1 min. Reactions were performed in triplicate with the ABI Prism 7700 Sequence Detection System (Applied Biosystems). Input RNA amounts were calculated with a multiplex comparative method for mRNAs of AM and 18S protein.

2.8. High-fat diet (HFD)

Male C57BL/6 mice aged 10 weeks were randomly divided into two groups, one fed a standard fat diet (11% fat by energy) and the other a high-fat diet (60% fat by energy, Research Diets, Inc., New Brunswick, NJ, USA). After 11 weeks, the retroperitoneal, subcutaneous, omental, epididymal white adipose tissue and kidney were removed and stored at −80 °C until total RNA preparation. Mouse plasma AM and leptin concentrations were determined with a radioimmunoassay (Phoenix Pharmaceuticals, Inc.) and an enzyme immunoassay (Immune Biological Laboratory, Gunma, Japan), respectively.

2.9. Statistical analysis

All data are expressed as the mean±S.E.M. Statistical analysis was performed with Student's t-test. Values of $P<0.05$ were considered to be statistically significant.

3. Results

3.1. AM gene expression in adipose tissue and mature adipocytes

The expression of AM gene was examined by means of Northern blotting (Fig. 1). A marked expression of AM mRNA was detected in all white adipose tissues from C57BL/6. The expression levels in the retroperitoneal, subcutaneous, omental, and epididymal adipose tissue were 3.2, 2.6, 2.5 and 2.7 times higher than the corresponding levels in the kidney. In addition to mature adipocytes, adipose tissue contains blood vessels, fibroblasts and preadipocytes, among which especially the vascular wall has been regarded as a site of AM production. We therefore separated the adipose tissue into a mature adipocytes fraction and sv-f, and examined AM expression in each fraction (Fig. 2). The AM mRNA level in the mature adipocyte

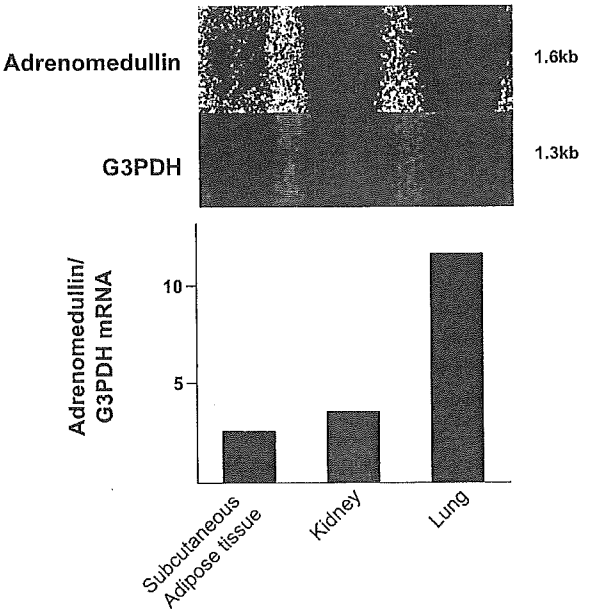

Fig. 3. Northern blot analysis of human AM mRNA content. 10 μg of total RNA in each lane was electrophoresed and hybridized with human AM cDNA probes. The lower panel indicates hybridization with a G3PDH probe as an internal control. The ratio of the AM to G3PDH mRNA is shown below.

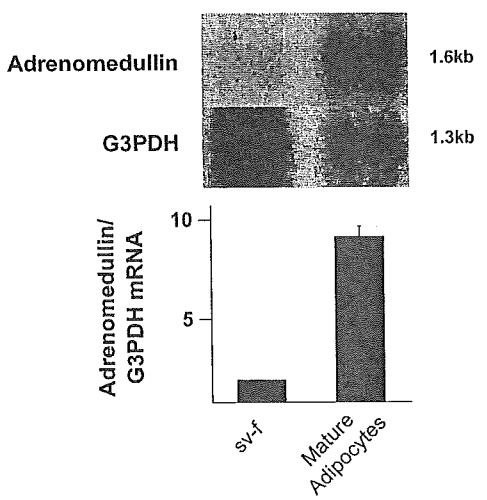

Fig. 2. Northern blot analysis of AM mRNA content in stroma–vascular fraction and isolated mature adipocytes of C3H/He mice. 10 μg of total RNA in each lane were electrophoresed and hybridized with mouse AM cDNA probes. The lower panel indicates hybridization with a G3PDH probe as an internal control. The ratio of AM to G3PDH mRNA is shown below. Bars represent the mean±S.E.M.

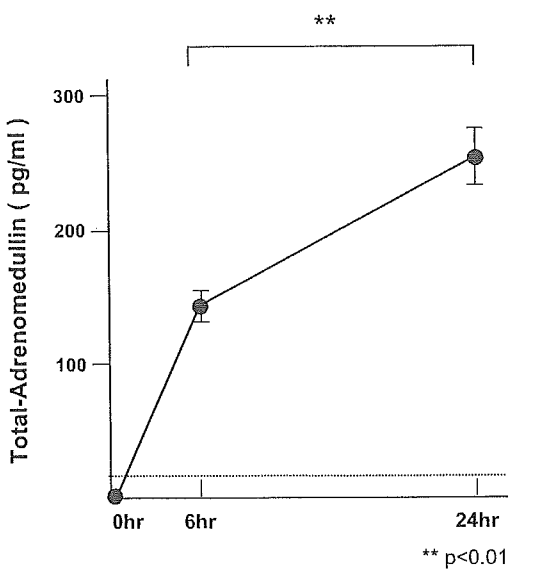

Fig. 4. Time course of AM levels in culture medium of mature adipocytes isolated from ICR mice (12 wk old, male, $n=5$). Mature adipocytes released AM, which significantly increased in a time-dependent manner. Bars represent the mean±S.E.M. Statistical analysis was performed with the t test. $^{**}P<0.01$.

Table 1
Body weight and plasma parameters in mice fed with high-fat diet or standard chow

	Standard chow	High-fat diet
Body weight(g)	31.3±1.2	48.6±2.1**
BS (mg/dl)	87.0±8.5	141.5±12.7**
FFA (mEq/ml)	0.51±0.08	0.94±0.18*
Leptin (ng/ml)	0.23±0.02	18.5±3.7***
Total AM (pg/ml)	56.3±17.5	84.9±6.2*

*$P<0.05$; **$P<0.01$, ***$P<0.001$ vs. standard chow group.

fraction was 7.3 times higher than that in the sv-f. In view of the tissue volume, this suggests that the major source of AM mRNA in the adipose tissue is mature adipocytes.

In the human subcutaneous adipose tissues obtained during plastic surgery, AM expression comparable to that in the kidney was detected (Fig. 3).

3.2. AM secretion from mature adipocytes

In addition to AM mRNA expression in the adipose tissue and mature adipocytes, we cultured mature adipocytes and measured AM peptide secretion in the medium. As shown in Fig. 4, AM peptide detected in the cultured medium increased in a time-dependent manner, indicating that AM is secreted from mature adipocytes.

3.3. Changes in AM gene expression in obesity

In order to assess the relationship between obesity and adipose AM production, we examined the AM mRNA expression after administration of the high-fat diet. As shown in Table 1, the HFD group weighed 1.5 times more than the standard chow group, and plasma leptin concentration was significantly higher as well as concentrations of plasma free fatty acid (FFA) and glucose. Plasma AM concentration in the HFD group was significantly higher than that in the standard chow group. After the high-fat diet, AM expression level was elevated in all adipose tissue compared with that in the control group, especially in retroperitoneal, subcutaneous and epididymal white adipose tissue (Fig. 5). In contrast, AM expression levels in the kidney of the HFD group and the control group were comparable.

In addition to HFD, we also examined AM mRNA expression in the obesity mouse model, ob/ob. Fig. 6 shows the AM mRNA level in the adipose tissues of ob/ob and the control, namely, C57BL/6 mice. In ob/ob mice, AM expression level was elevated in all adipose tissues compared with that in C57BL/6, especially in subcutaneous, omental, epididymal white adipose tissue and BAT.

4. Discussion

AM has been implicated in the regulation of circulation and the development of vasculature. Although AM was originally isolated from pheochromocytoma cells, the major site of production in the physiological state is believed to be vascular endothelial cells. Our findings demonstrate that adipose tissue strongly expresses the AM gene. In C57BL/6 mice, AM mRNA expression in all white adipose tissues examined was found to be higher than that detected in kidney. Adipose tissue is capillary-rich, containing blood vessels, fibroblasts and preadipocytes in addition to mature adipocytes. In order to exclude the possibility that AM mRNA in the adipose tissue is of vascular endothelial cell origin, we examined the AM expression in the mature adipocyte fraction and sv-f separately and found that the AM mRNA level in the mature adipocyte fraction was much higher than that in the sv-f, which consists of small vessels, preadipocytes and connective tissue. Moreover, we determined AM peptide secretion from isolated mature adipocytes in the medium. These findings indicate that the major source of AM in the adipose tissue consists of mature adipocytes. A few reports about adipose tissue and AM have

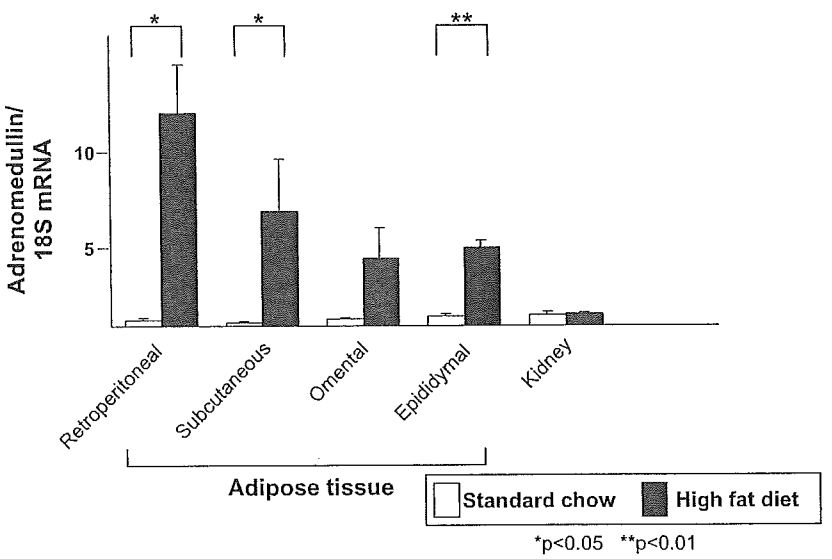

Fig. 5. AM mRNA levels from C57BL/6 mice (21 wk old, male, $n=5$) after 11 weeks of standard chow diet (open bars) or high-fat diet (closed bars). Bars represent the mean±S.E.M. Statistical analysis was performed with the t test. *$P<0.05$; **$P<0.01$.

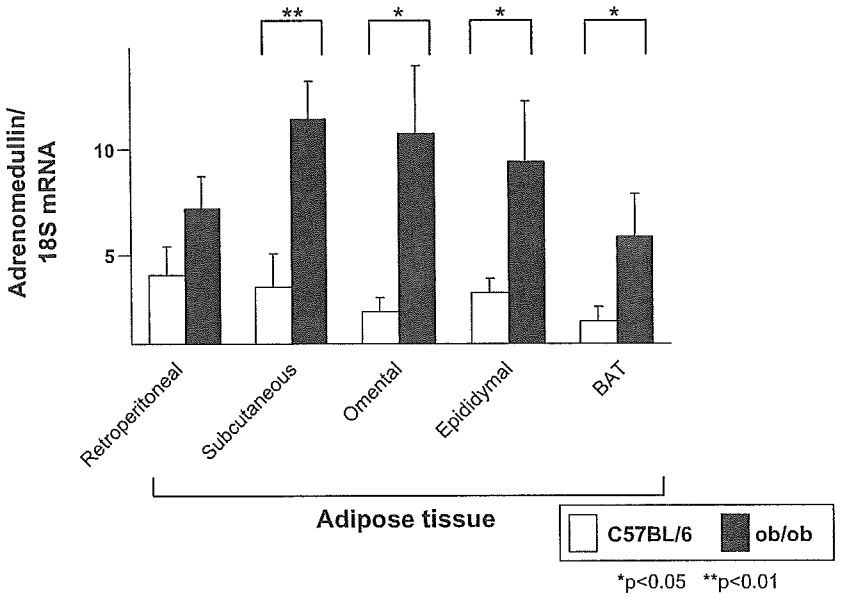

Fig. 6. AM mRNA levels in C57BL/6 (open bars) and ob/ob mice (closed bars) (14 wk old, male, $n=5$). Bars represent the mean±S.E.M. Statistical analysis was performed with the t test. $^{*}P<0.05$; $^{**}P<0.01$.

been published. Using NIH 3T3-L1 cells, Li et al. reported observing AM mRNA expression and secretion in mature adipocytes [14,15]. Recently Fukai et al. found AM mRNA expression in rat and human adipose tissue [16], which agrees with the results of our study.

Human subcutaneous adipose tissue obtained from healthy subjects during plastic surgery exhibited marked AM expression, too. In view of the tissue volume, these results suggest that adipose tissue is one of the major sites of AM production in the body.

The physiological significance of adipocyte-derived AM remains to be clarified. Since it has been reported that the plasma concentration of AM in the physiological state is not high enough to exert a vasodilatory effect [17], it stands to reason that AM secreted from adipocytes functions in an autocrine/paracrine manner. Adipose tissue is distributed throughout the body and works as supportive tissue. AM is a potent vasodilator and a growth factor for vascular endothelial cells (VEC) and vascular smooth muscle cells (VSMC) [18,19]. Many blood vessels are surrounded by fat and AM produced by the adipocytes and the vascular wall itself may make the local concentration of AM high enough to work as a vasodilator or a growth factor for VEC and VSMC. In reconstruction culture of the skin, the epidermal layer is known to grow better on the subcutaneous adipose layer [20]. It has also been reported that AM has a mitogenic effect on human keratinocytes [21]. Along with its enhancing effect on the proliferation and migration of VEC and VSMC, AM secreted from subcutaneous adipose tissue may be crucial for the maintenance and regeneration of the skin. Bone marrow is another organ which is rich in adipose tissue, while it has been reported that AM is expressed in cord blood hematopoietic cells and stimulates their clonal growth [22]. It thus seems reasonable to speculate that bone marrow fat may contribute to haematopoiesis.

It is extremely interesting that AM expression in adipose tissue and plasma AM concentration were significantly augmented with the increase in body weight after the high-fat diet. The same results were observed in ob/ob, leptin-deficient obesity model mice [23]. Furthermore, the massive increase in adipose tissue volume in obesity makes the total AM production in adipose tissue much greater. It has also been reported that the expression of the AM receptor components CRLR and RAMP2 was heightened in HFD rat adipose tissue [16]. Shimosawa et al. reported that heterozygous AM-deficient mice showed obesity, higher blood pressure and insulin resistance in their old age [24]. Taken together, these findings suggest that adipose tissue-derived AM protects against obesity.

The relationship between human plasma AM levels and obesity is not clear yet, although several studies have shown that plasma human AM levels are elevated in obesity [25,26].

In conclusion, our study presented here demonstrated that adipocytes produce AM in human and mouse and the AM production in adipose tissue is enhanced in obesity. Adipose AM may thus have a pathophysiological function in obesity.

Acknowledgements

This study was supported in part by the Smoking Research Foundation.

References

[1] Ahima RS, Flier JS. Adipose tissue as an endocrine organ. Trends Endocrinol Metab 2000;11:327–32.
[2] Janke J, Engeli S, Gorzelniak K, Luft FC, Sharma AM. Mature adipocytes inhibit in vitro differentiation of human preadipocytes via angiotensin type 1 receptors. Diabetes 2002;51:1699–707.

[3] Hauner H, Petruscheke T, Gries FA. Endothelin-1 inhibits the adipose differentiation of cultured human adipocyte precursor cells. Metabolism 1994;43:227–32.
[4] Nisoli E, Clementi E, Tonello C, Sciorati C, Brinscini L, Carruba MO. Effects of nitric oxide on proliferation and differentiation of rat brown adipocytes in primary cultures. Br J Pharmacol 1998;125:888–94.
[5] Aubert J, Saint-Marc P, Belmonte N, Dani C, Negrel R, Ailhaud G. Prostacyclin IP receptor up-regulates the early expression of C/EBPbeta and C/EBPdelta in preadipose cells. Mol Cell Endocrinol 2000;16: 149–56.
[6] Sengenes C, Berlan M, De Glisezinski I, Lafontan M, Galitzky J. Natriuretic peptides: a new lipolytic pathway in human adipocytes. FASEB J 2000;14:1345–51.
[7] Kitamura K, Kangawa K, Kawamoto M, Ichiki Y, Nakamura S, Matsuo H, Eto T. Adrenomedullin: a novel hypotensive peptide isolated from human pheochromocytoma. Biochem Biophys Res Commun 1993;192:553–60.
[8] McLatchie LM, Fraser NJ, Main MJ, Wise A, Brown J, Thompson N, Solari R, Lee MG, Foord SM. RAMPs regulate the transport and ligand specificity of the calcitonin-receptor-like receptor. Nature 1998;393: 333–9.
[9] Washimine H, Kitamura K, Ichiki Y, Yamamoto Y, Kangawa K, Masuo H, Eto T. Immunoreactive proadrenomedullin N-terminal 20 peptide in human tissue, plasma and urine. Biochem Biophys Res Commun 1994; 202:1081–7.
[10] Sugo S, Minamino N, Shoji H, Kangawa K, Kitamura K, Eto T, Matsuo H. Interleukin-1, tumor necrosis factor and lipopolysaccharide additively stimulate production of adrenomedullin in vascular smooth muscle cells. Biochem Biophys Res Commun 1995;207:25–32.
[11] Nagae T, Mukoyama M, Sugawara A, Mori K, Yahata K, Kasahara M, Suganami T, Makino H, Fujinaga Y, Yoshioka T, Tanaka I, Nakao K. Rat receptor-activity-modifying proteins (RAMPs) for adrenomedullin/CGRP receptor: cloning and upregulation in obstructive nephropathy. Biochem Biophys Res Commun 2000;270:89–93.
[12] Rodbell M. Metabolism of isolated fat cells. J Biol Chem 1964; 239:375–80.
[13] Cassis LA, English VL, Bharadwaj K, Boustany CM. Differential effects of local versus systemic angiotensin II in the regulation of leptin release from adipocytes. Endocrinology 2004;145:169–74.
[14] Li Y, Totsune K, Takeda K, Furuyama K, Shibahara S, Takahashi K. Decreased expression of adrenomedullin during adipocyte-differentiation of 3T3-L1 cells. Hypertens Res 2003;26:S41–4.
[15] Li Y, Totsune K, Takeda K, Furuyama K, Shibahara S, Takahashi K. Differential expression of adrenomedullin and resistin in 3T3-L1 adipocytes treated with tumor necrosis factor-alpha. Eur J Endocrinol 2003; 149:231–8.
[16] Fukai N, Yoshimoto T, Sugiyama T, Ozawa N, Sato R, Shichiri M, Hirata Y. Concominant expression of adrenomedullin and its receptor components in rat adipose tissues. Am J Physiol Endocrionol Metab 2005;288: E56–62.
[17] Shindo T, Kurihara H, Maemura K, Kurihara Y, Kuwaki T, Izumida T, Minamino N, Ju KH, Morita H, Oh-hashi Y, Kumada M, Kangawa K, Nagai R, Yazaki Y. Hypotension and resistance to lipopolysaccharide-induced shock in transgenic mice overexpressing adrenomedullin in their vasculature. Circulation 2000;101:2309–16.
[18] Shichiri M, Fukai N, Ozawa N, Iwasaki H, Hirata Y. Adrenomedullin is an autocrine/paracrine growth factor for rat vascular smooth muscle cells. Regul Pept 2003;112:167–73.
[19] Miyashita K, Itoh H, Sawada N, Fukunaga Y, Sone M, Yamahara K, Yurugi T, Nakao K. Adrenomedullin promotes proliferation and migration of cultured endothelial cells. Hypertens Res 2003;26:S93–8.
[20] Sugihara H, Toda S. Reconstruction culture of the skin. In: Doyle A, editor. Cell & tissue culture: laboratory procedures. Chichester: John Wiley & Sons Company Ltd.; 1995. p. 3A 2.1-2.12.
[21] Kapas S, Brown DW, Farthing PM, Hagi-Pavli E. Adrenomedullin has mitogenic effects on human oral keratinocytes: involvement of cyclic AMP. FEBS Lett 1997;418:287–90.
[22] Del Pup L, Belloni AS, Carraro G, De Angeli S, Parnigotto PP, Nussdorfer GG. Adrenomedullin is expressed in cord blood hematopoietic cells and stimulates their clonal growth. Int J Mol Med 2003;11:157–60.
[23] Pelleymounter MA, Cullen MJ, Baker MB, Hecht R, Winters D, Boone T, Collins F. Effects of the obese gene product on body weight regulation in ob/ob mice. Science 1995;269:540–3.
[24] Shimosawa T, Ogihara T, Matsui H, Asano T, Ando K, Fujita T. Deficiency of adrenomedullin induces insulin resistance by increasing oxidative stress. Hypertension 2003;41:1080–5.
[25] Minami J, Nishikimi T, Ishimitsu T, Makino Y, Kawano Y, Takishita S, Kangawa K, Matsuoka H. Effect of a hypocaloric diet on adrenomedullin and natriuretic peptides in obese patients with essential hypertension. J Cardiovasc Pharmacol 2000;36:S83–6.
[26] Kato J, Kitamura K, Uemura T, Kuwasako K, Kita T, Kangawa K, Eto T. Plasma levels of adrenomedullin and atrial and brain natriuretic peptides in the general population: their relations to age and pulse pressure. Hypertens Res 2002;25:887–92.

CASE REPORT

Spontaneous regression of congenital cystic adenomatoid malformation of the lung: Longitudinal examinations by magnetic resonance imaging

Makoto Kawamura, Hiroaki Itoh, Shigehito Yamada, Shigeo Yura, Satoko Katsuya, Kenzo Kosaka, Keiji Tatsumi, Junzo Hamanishi, Ayako Suzuki, and Shingo Fujii

Department of Gynecology and Obstetrics, Kyoto University Graduate School of Medicine, 54 Shogoin Kawahara-cho, Sakyo-ku, Kyoto 606-8507, Japan

ABSTRACT **We report a case of large cystic adenomatoid malformation of the lung (CCAM), which occupied almost the entire left lung with a prominent mediastinal shift at 24 weeks of gestation. The volume of the lesion, determined by magnetic resonance imaging (MRI), was 27.0 cm^3. Subsequent MRI and ultrasound examinations revealed a spontaneous resolution of the lesion at 32 and 36 weeks of gestation without a mediastinal shift, when the lesion volume was 12.8 cm^3 and 5.6 cm^3, respectively. At 37 weeks of gestation, a mature male baby weighing 2638 g with an Apgar score of 7 was delivered by elective cesarean section. A lobectomy of the left upper lobe of the lung was carried out at 3 days of age, due to an enlargement of the CCAM after birth.**

Key Words: congenital cystic adenomatoid malformation, magnetic resonance imaging, pregnancy, prenatal diagnosis, spontaneous remission

INTRODUCTION

A congenital cyctic adenomatoid malformation (CCAM) is a rare congenital pulmonary lesion, with a reported incidence ranging from 1 in 25 000–35 000 pregnancies (Laberge *et al.* 2001), involving maldevelopment of terminal branches, as a consequence of an abnormal embryogenesis during the first 6–7 weeks of pregnancy (Stocker *et al.* 1977; Adzick *et al.* 1985). Although disorders in Hoxb5 and/or FGF7 genes were reported to be possibly associated with CCAM development (Groenman *et al.* 2005), the entire molecular basis for CCAM development is yet to be clarified.

In 1977, Stocker *et al.* demonstrated three types of classification in CCAM according to the clinical and pathologic features (Stocker *et al.* 1977). Stocker recently added two more types and used the term 'congenital pulmonary airway malformation', based on anatomic and microscopic features of the pulmonary airways (Stocker 2002). Pulmonary hypoplasia and/or heart failure may be associated with polyhydroamnios, a mediastinal shift, and especially non-immune fetal hydrops (NIFH) (Olson & Mendelsohn 1978; Ostor & Fortune 1978; Miller *et al.* 1996; De Santis *et al.* 2000). However, in rare cases, spontaneous regression or resolution of the lesion *in utero* can occur (Sakala *et al.* 1994; Hsu *et al.* 1995; Miller *et al.* 1996; Dommergues *et al.* 1997; Higby *et al.* 1998; Bagolan *et al.* 1999; De Santis *et al.* 2000; Duncombe *et al.* 2002; Kahler *et al.* 2002; Diamond *et al.* 2003; Pumberger *et al.* 2003). Recently, prenatal magnetic resonance imaging (MRI) with new ultrafast imaging sequences was introduced in the diagnosis and management of CCAM (Quinn *et al.* 1998; Hubbard & States 2001; Kuga *et al.* 2001; Breysem *et al.* 2003; Castanon *et al.* 2003; Matsuoka *et al.* 2003; Morikawa *et al.* 2003; Robert *et al.* 2003). We present a case of spontaneous regression of CCAM which was longitudinally assessed by estimating net lesion volume with MRI.

CASE REPORT

The patient was a 34-year-old woman (gravid, 0; parous, 0) without any history of previous disease. Her relatives had no history of congenital anomalies. At 21 weeks of gestation, an ultrasound examination detected a microcystic lesion in the left fetal lung and the patient was referred to Kyoto University Hospital at 23 weeks of gestation for further diagnosis and management of delivery. Both ultrasound (Fig. 1A) and MRI (Fig. 1B) examinations at 24 weeks of gestation showed a multimicrocystic lesion occupying the entire left fetal lung, which caused a prominent mediastinal shift, suggesting CCAM type II of the left fetal lung (Stocker *et al.* 2002). The MRI revealed the CCAM to have a volume of 27.0 cm^3 (Fig. 2). The blood flow in the left fetal pulmonary artery was below the limit of sensitivity to color Doppler ultrasound examinations, probably due to direct compression by the CCAM. The ultrasound examination detected no other structural abnormalities in the fetus and fetal growth was estimated to be within the normal range. Subsequent ultrasound (Fig. 1C) and MRI (Fig. 1D) examinations at 30 weeks of gestation detected the CCAM only in the upper lobe of the left fetal lung without mediastinal shift. The lesion volume was 12.8 cm^3 by MRI (Fig. 2) and pulmonary artery blood flow was well observed. At 36 weeks of gestation, the lesion had shrunk (Figs 1E,F) 5.6 cm^3 (Fig. 2). Then elective cesarean section was carried out at 37 weeks of gestation in order to prepare for possible respiratory disorders soon after delivery and a mature male baby weighing 2638 g was born with an Apgar score of 7. At opening of the thoracic cavity, bulging of upper lobe of the left lung, with multiple cystic lesions, was observed. Then, a lobectomy of the upper lobe of the left lung was carried out at 3 days of age, due to enlargement of the CCAM after birth. Figure 3A shows the cystic surface of the lobe (Fig. 3A). Histological examination revealed a mixture of both terminal bronchiole-like structure and alveolus-like structure (Fig. 3B). Diameters of cysts ranged approximately from 6 mm to 2 cm. Gross appearance was not solid. These findings were compatible with CCAM type II (Stocker *et al.* 2002).

Correspondence: Hiroaki Itoh, MD, D Med Sci, Department of Gynecology, Obstetrics, Kyoto University Graduate School of Medicine, 54 Shogoin Kawahara-cho, Sakyo-ku, Kyoto 606-8507, Japan.
Email: ihiroaki@kuhp.kyoto-u.ac.jp

Received July 19, 2005; revised and accepted August 29, 2005.

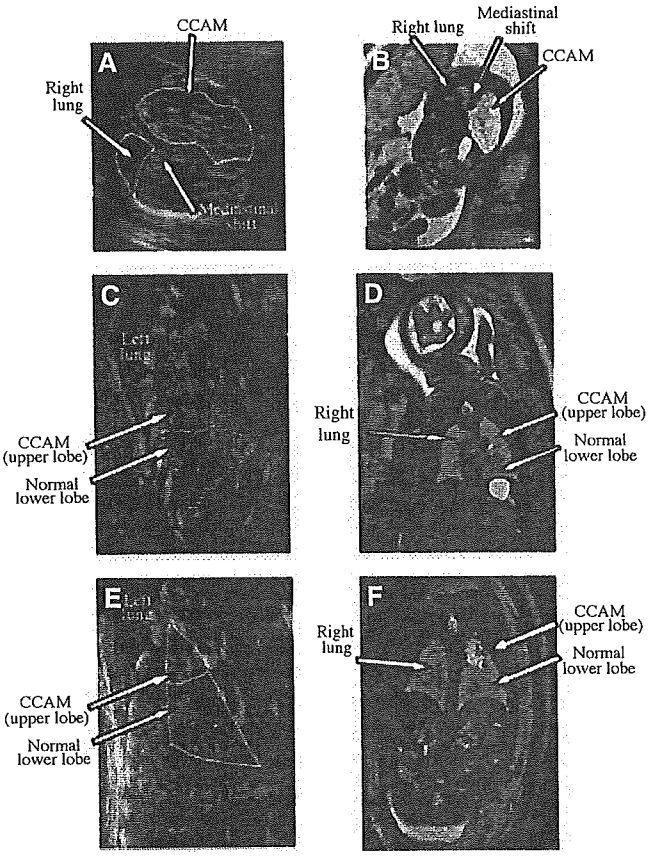

Fig. 1 Ultrasound (**A, C, E**) and MR (T2-weighted, **B, D, F**) images at 24 (**A, C**), 30 (**C, D**), and 36 (**E, F**) weeks of gestation.

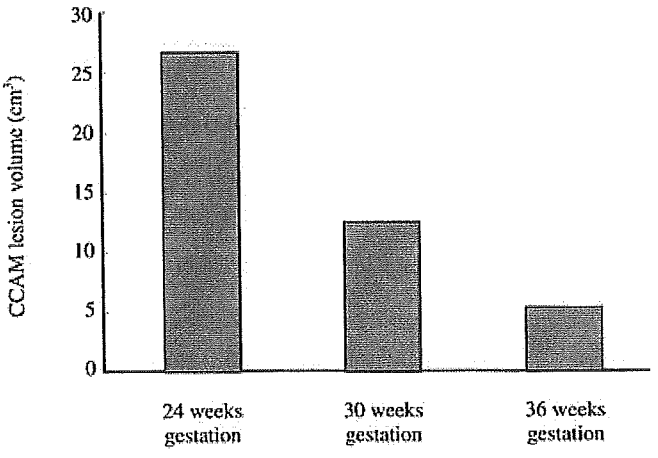

Fig. 2 Estimated volume of the CCAM at 24, 30, and 36 weeks of gestation. Columns indicate net volume of the lesion measured by MRI.

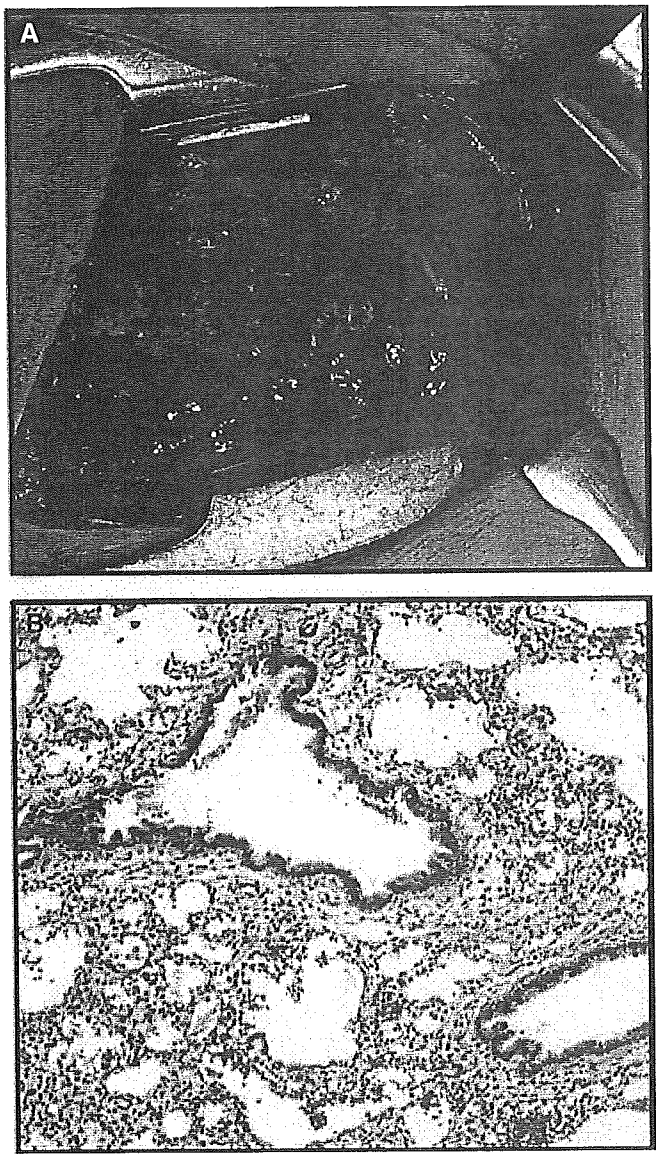

Fig. 3 Surface appearance of the CCAM during the operation 3 days after birth (**A**) and pathological findings of the lesion (**B**) (Hematoxylin and eosin staining, original magnification was × 200).

DISCUSSION

First reported in 1949 (Chin & Tang 1949), CCAM is a rare hamartoma of the lung caused by a maldevelopment of the terminal bronchioli, which become hyperplastic without developing a normal alveolar structure (Stocker *et al.* 1977; Adzick *et al.* 1985). Prenatally, it is detected as an echogenic lesion within the thorax on ultrasound scan, and the diagnostic criteria for CCAM are enlargement of the affected lung with either hyperechogenicity or cystic appearance (King *et al.* 1995). NIFH is considered to be an indicator of an ominous outcome in cases of CCAM, which is caused by either obstruction of venous return to the heart or direct compression of the heart by the lesion (Rice *et al.* 1994; Mahle *et al.* 2000). Rice *et al.* showed that elevating intrathoracic pressure by inflating an expander in fetal sheep-caused hydrops was resolved after deflation of the expander (Rice *et al.* 1994). Therefore, mediastinal shift by CCAM, as was observed in the present case at 24 weeks of gestation, is potentially an unfavorable causative factor of further development of NIFH. However, intervention *in utero* was not carried out at that point in the pregnancy, because NIFH was not detected for all an apparent mediastinal shift with an absence of blood flow in the left fetal pulmonary artery (Adzick *et al.* 1993; Morin *et al.* 1994).

Postnataly, CCAM may result in early neonatal death from pulmonary hypoplasia, mild to severe neonatal respiratory distress, or repeated infectious complications during the infantile period, while in rare cases it is asymptomatic (van Leeuwen *et al.* 1999). Previously, the option of terminating the pregnancy was usually offered if ultrasound examination revealed a suspected CCAM lesion (Roelofsen *et al.* 1994); however, Schwartz (Schwartz & Ramachandran 1997) and Nuchtern (Nuchtern & Harberg 1994) demonstrated that the general prognosis of CCAM, prenataly diagnosed by ultrasound examination, was not so bad. Indeed, even spontaneous regression or remission of CCAM, as in this case, has been reported (McCullagh *et al.* 1994; Sakala *et al.* 1994; Hsu *et al.* 1995; Miller *et al.* 1996; Dommergues *et al.* 1997; Higby *et al.* 1998; Bagolan *et al.* 1999; De Santis *et al.* 2000; Duncombe *et al.* 2002; Kahler *et al.* 2002; Diamond *et al.* 2003; Pumberger *et al.* 2003). However, it is not clear exactly how often CCAM regresses spontaneously *in utero*. Diamond *et al.* reported nine cases of CCAM in which there was a spontaneous resolution of hydrops, a progression of the pregnancy to term, and postnatal survival by reviewing the literature from 1980 to 2000 (Diamond *et al.* 2003). One difficulty with these reports was a lack of longitudinal evaluation of the net volume of the CCAM, in addition to no final confirmation of the pathological diagnosis.

MRI has been reported to be useful in the prenatal differential diagnosis of CCAM (Quinn *et al.* 1998; Hubbard *et al.* 1999). The introduction of ultrafast scanning, taking less than one second allows obtaining clear images for all vigorous fetal movements (Levine *et al.* 1996; Wagenvoort *et al.* 2000). Therefore MRI examination has played an important role in the further characterization of various fetal thoracic lesions including CCAM (Williams & Johnson 2002; Castanon *et al.* 2003; Matsuoka *et al.* 2003; Morikawa *et al.* 2003), in cooporation with ultrasound examination, which has a great advantage in clinical screening. Moreover, we longitudinally estimated the volume of the CCAM, by MRI data, using image analysis sotware NIHimage, version 1.63. The net volume of the lesion was estimated to be reduced (Fig. 3), directly indicating spontaneous regression *in utero*. Spontaneous regression or remission of CCAM *in utero* has been reported previously (Sakala *et al.* 1994; Hsu *et al.* 1995; Miller *et al.* 1996; Dommergues *et al.* 1997; Higby *et al.* 1998; Bagolan *et al.* 1999; De Santis *et al.* 2000; Duncombe *et al.* 2002; Kahler *et al.* 2002; Diamond *et al.* 2003; Pumberger *et al.* 2003). But these reports lacked final histological confirmation. Van Leeuwen *et al.* revealed that no further remission of CCAM was evident in the neonatal period following a partial resolution *in utero* (van Leeuwen *et al.* 1999). In the present case, an enlargement of the CCAM of unknown etiology was observed soon after birth and a lobectomy was carried out. The histology of the removed tissues was compatible with CCAM. Intensive histological examination could not detect findings to explain rapid enlargement of the CCAM after birth. We have no clear explanation for the enlargement after birth. Thus, in the present case, prenatal analyzes of volume based on MRI and postnatal histology, together, proved the spontaneous regression of CCAM *in utero*.

In summary, we reported a case of spontaneous regression of CCAM *in utero*. Consecutive prenatal analyzes of the lesion's volume by MRI were useful to estimate the course of partial remission of the CCAM.

ACKNOWLEDGMENTS

The authors also acknowledge Ms. Sachiko Kohama for secretarial assistance with this work.

REFERENCES

Adzick NS, Harrison MR, Flake AW, Howell LJ, Golbus MS, Filly RA (1993) Fetal surgery for cystic adenomatoid malformation of the lung. *J Pediatr Surg* **28**: 806–812.

Adzick NS, Harrison MR, Glick PL *et al.* (1985) Fetal cystic adenomatoid malformation: Prenatal diagnosis and natural history. *J Pediatr Surg* **20**: 483–488.

Bagolan P, Nahom A, Giorlandino C *et al.* (1999) Cystic adenomatoid malformation of the lung: Clinical evolution and management. *Eur J Pediatr* **158**: 879–882.

Breysem L, Bosmans H, Dymarkowski S *et al.* (2003) The value of fast MR imaging as an adjunct to ultrasound in prenatal diagnosis. *Eur Radiol* **13**: 1538–1548.

Castanon M, Munoz ME, San Vicente B, Albert A, Tarrado X, Morales L (2003) Predictive value of prenatal MRI in the diagnosis of thoracic congenital malformations. *Cir Pediatr* **16**: 107–111.

Chin Y, Tang M (1949) Congenital adenomatoid malformation of one lobe of a lung with general anasarca. *Arch Pathol* **61**: 221–229.

De Santis M, Masini L, Noia G, Cavaliere AF, Oliva N, Caruso A (2000) Congenital cystic adenomatoid malformation of the lung: Antenatal ultrasound findings and fetal-neonatal outcome. Fifteen years of experience. *Fetal Diagn Ther* **15**: 246–250.

Diamond IR, Wales PW, Smith SD, Fecteau A (2003) Survival after CCAM associated with ascites: A report of a case and review of the literature. *J Pediatr Surg* **38**: E1–E3.

Dommergues M, Louis-Sylvestre C, Mandelbrot L *et al.* (1997) Congenital adenomatoid malformation of the lung: When is active fetal therapy indicated? *Am J Obstet Gynecol* **177**: 953–958.

Duncombe GJ, Dickinson JE, Kikiros CS (2002) Prenatal diagnosis and management of congenital cystic adenomatoid malformation of the lung. *Am J Obstet Gynecol* **187**: 950–954.

Groenman F, Unger S, Post M (2005) The molecular basis for abnormal human lung development. *Biol Neonate* **87**: 164–177.

Higby K, Melendez BA, Heiman HS (1998) Spontaneous resolution of nonimmune hydrops in a fetus with a cystic adenomatoid malformation. *J Perinatol* **18**: 308–310.

Hsu KF, Wu MH, Chang CH, Yao BL, Chang FM (1995) Complete intrauterine resolution of fetal congenital cystic adenomatoid malformation of the lung type III. *J Ultrasound Med* **14**: 871–875.

Hubbard AM, Adzick NS, Crombleholme TM *et al.* (1999) Congenital chest lesions: Diagnosis and characterization with prenatal MR imaging. *Radiology* **212**: 43–48.

Hubbard AM, States LJ (2001) Fetal magnetic resonance imaging. *Top Magn Reson Imaging* **12**: 93–103.

Kahler C, Schulze E, Eichhorn KH, Seewald HJ (2002) Fetal hyperechogenic and cystic pulmonary masses: Sonographic findings, antenatal management and outcome of 12 cases. *Z Geburtshilfe Neonatol* **206**: 205–210.

King SJ, Pilling DW, Walkinshaw S (1995) Fetal echogenic lung lesions: Prenatal ultrasound diagnosis and outcome. *Pediatr Radiol* **25**: 208–210.

Kuga T, Inoue T, Sakano H, Zempo N, Oga A, Esato K (2001) Congenital cystic adenomatoid malformation of the lung with an esophageal cyst: Report of a case. *J Pediatr Surg* **36**: E4.

Laberge JM, Flageole H, Pugash D *et al.* (2001) Outcome of the prenatally diagnosed congenital cystic adenomatoid lung malformation: A Canadian experience. *Fetal Diagn Ther* **16**: 178–186.

Levine D, Hatabu H, Gaa J, Atkinson MW, Edelman RR (1996) Fetal anatomy revealed with fast MR sequences. *Am J Roentgenol* **167**: 905–908.

Mahle WT, Rychik J, Tian ZY *et al.* (2000) Echocardiographic evaluation of the fetus with congenital cystic adenomatoid malformation. *Ultrasound Obstet Gynecol* **16**: 620–624.

Matsuoka S, Takeuchi K, Yamanaka Y, Kaji Y, Sugimura K, Maruo T (2003) Comparison of magnetic resonance imaging and ultrasonography in the prenatal diagnosis of congenital thoracic abnormalities. *Fetal Diagn Ther* **18**: 447–453.

McCullagh M, MacConnachie I, Garvie D, Dykes E (1994) Accuracy of prenatal diagnosis of congenital cystic adenomatoid malformation. *Arch Dis Child* **71**: F111–F113.

Miller JA, Corteville JE, Langer JC (1996) Congenital cystic adenomatoid malformation in the fetus: Natural history and predictors of outcome. *J Pediatr Surg* **31**: 805–808.

Morikawa M, Yamada H, Okuyama K *et al.* (2003) Prenatal diagnosis and fetal therapy of congenital cystic adenomatoid malformation type I of the lung: A report of five cases. *Congenit Anom Kyoto* **43**: 72–78.

Morin L, Crombleholme TM, D'Alton ME (1994) Prenatal diagnosis and management of fetal thoracic lesions. *Semin Perinatol* **18**: 228–253.

Nuchtern JG, Harberg FJ (1994) Congenital lung cysts. *Semin Pediatr Surg* **3**: 233–243.

Olson JL, Mendelsohn G (1978) Congenital cystic adenomatoid malformation of the lung. *Arch Pathol Lab Med* **102**: 248–251.

Ostor AG, Fortune DW (1978) Congenital cystic adenomatoid malformation of the lung. *Am J Clin Pathol* **70**: 595–604.

Pumberger W, Hormann M, Deutinger J, Bernaschek G, Bistricky E, Horcher E (2003) Longitudinal observation of antenatally detected congenital lung malformations (CLM): Natural history, clinical outcome and long-term follow-up. *Eur J Cardiothorac Surg* **24**: 703–711.

Quinn TM, Hubbard AM, Adzick NS (1998) Prenatal magnetic resonance imaging enhances fetal diagnosis. *J Pediatr Surg* **33**: 553–558.

Rice HE, Estes JM, Hedrick MH, Bealer JF, Harrison MR, Adzick NS (1994) Congenital cystic adenomatoid malformation: A sheep model of fetal hydrops. *J Pediatr Surg* **29**: 692–696.

Robert Y, Cuilleret V, Vaast P *et al.* (2003) Fetal thoracic MR imaging. *Arch Pediatr* **10**: 340–346.

Roelofsen J, Oostendorp R, Volovics A, Hoogland H (1994) Prenatal diagnosis and fetal outcome of cystic adenomatoid malformation of the lung: Case report and historical survey. *Ultrasound Obstet Gynecol* **4**: 78–82.

Sakala EP, Furness ME, Perrott WS, Grube GL (1994) Spontaneous, in utero regression of antenatally diagnosed solid fetal chest masses. A report of two cases. *J Reprod Med* **39**: 531–536.

Schwartz MZ, Ramachandran P (1997) Congenital malformations of the lung and mediastinum – a quarter century of experience from a single institution. *J Pediatr Surg* **32**: 44–47.

Stocker JT (2002) Congenital pulmonary airway malformation: A new name and an expanded classification of congenital cystic adenomatoid malformations of the lung. *Histopathology* **41**: 424–431.

Stocker JT, Madewell JE, Drake RM (1977) Congenital cystic adenomatoid malformation of the lung. Classification and morphologic spectrum. *Hum Pathol* **8**: 155–171.

Van Leeuwen K, Teitelbaum DH, Hirschl RB *et al.* (1999) Prenatal diagnosis of congenital cystic adenomatoid malformation and its postnatal presentation, surgical indications, and natural history. *J Pediatr Surg* **34**: 794–798; discussion 798–799.

Wagenvoort AM, Bekker MN, Go AT *et al.* (2000) Ultrafast scan magnetic resonance in prenatal diagnosis. *Fetal Diagn Ther* **15**: 364–372.

Williams HJ, Johnson KJ (2002) Imaging of congenital cystic lung lesions. *Paediatr Respir Rev* **3**: 120–127.